



Published in final edited form as:

Circulation. 2014 February 4; 129(5): 598–606. doi:10.1161/CIRCULATIONAHA.113.002562.

The Role of Extracellular RNA in Atherosclerotic Plaque Formation in Mice

Sakine Simsekylmaz, PhD^{1,*}, Hector A. Cabrera-Fuentes, MSc^{2,3,*}, Svenja Meiler, PhD⁴, Sawa Kostin, PhD, MD⁵, Yvonne Baumer, PhD⁴, Elisa A. Liehn, MD, PhD¹, Christian Weber, MD^{6,7}, William A. Boisvert, PhD⁴, Klaus T. Preissner, PhD^{2,**}, and Alma Zerneck, MD^{7,8,9,**}

¹Institute for Molecular Cardiovascular Research, RWTH University Hospital Aachen, Aachen, Germany

²Department of Biochemistry, Medical School, Justus-Liebig-University, Giessen, Germany

³Department of Microbiology, Kazan Federal University, Kazan, Russian Federation

⁴Center for Cardiovascular Research, John A. Burns School of Medicine, University of Hawaii, Honolulu, HI

⁵Core Lab for Molecular and Structural Biology, Max-Planck-Institute for Heart and Lung Research, Bad Nauheim, Germany

⁶Institute for Cardiovascular Prevention, Ludwig-Maximilians-University, Munich, Germany

⁷DZHK (German Centre for Cardiovascular Research), partner site Munich Heart Alliance, Munich, Germany

⁸Rudolf Virchow Center and Institute of Clinical Biochemistry and Pathobiochemistry, University of Würzburg, 97080 Würzburg, Germany

⁹Department of Vascular Surgery, Klinikum rechts der Isar, Technical University, Munich, Germany

Abstract

Background—Atherosclerosis and vascular remodeling after injury are driven by inflammation and mononuclear cell infiltration. Extracellular RNA (eRNA) has recently been implicated to become enriched at sites of tissue damage, and to act as a pro-inflammatory mediator. We here addressed the role of eRNA in high-fat-diet (HFD)-induced atherosclerosis and neointima formation after injury in atherosclerosis-prone mice.

Methods and Results—The presence of eRNA was revealed in atherosclerotic lesions from HFD-fed low density lipoprotein receptor-deficient (*Ldlr*^{-/-}) mice in a time-progressive fashion. RNase activity in plasma increased within the first 2 weeks (44 ± 9 vs. 70 ± 7 mU/mg protein; p=0.0012), followed by a decrease to levels below baseline after 4 weeks of HFD (44 ± 9 vs. 12 ± 2 mU/mg protein; p<0.0001). Exposure of bone marrow-derived macrophages to eRNA resulted in a concentration-dependent upregulation of the pro-inflammatory mediators tumor necrosis factor- α , arginase-2, Interleukin (IL)-1 β , IL-6 and Interferon- γ . In a model of accelerated atherosclerosis after arterial injury in apolipoprotein E-deficient (*apoE*^{-/-}) mice, treatment with

Correspondence: Alma Zerneck, MD, Klinikum rechts der Isar, TUM, Klinik für Gefäßchirurgie, Ismaninger Strasse 22, D-81675 München, Germany, Phone: +49-89-4140-2167, Fax: +49-89-4140-4861, zerneck@lrz.tum.de.

*equal contribution as first authors

**equal contribution as senior authors

Conflict of Interest Disclosures: None.

RNase1 diminished the increased plasma level of eRNA, evidenced after injury. Likewise, RNase1 administration reduced neointima formation compared to vehicle-treated *apoE*^{-/-} controls (25.0 ± 6.2 vs. $46.9 \pm 6.9 \times 10^3 \mu\text{m}^2$, $p=0.0339$), and was associated with a significant decrease in plaque macrophage content. Functionally, RNase1 treatment impaired monocyte arrest on activated smooth muscle cells under flow conditions *in vitro*, and inhibited leukocyte recruitment to injured carotid arteries *in vivo*.

Conclusions—As eRNA is associated with atherosclerotic lesions and contributes to inflammation-dependent plaque progression in atherosclerosis-prone mice, its targeting with RNase1 may serve as a new treatment option against atherosclerosis.

Keywords

vascular biology; atherosclerosis; inflammation; nucleic acid

Introduction

Atherosclerosis and its sequelae are the most frequent cause of death in Western societies. The continuing age-related narrowing of (coronary) arteries can necessitate the need for percutaneous transluminal angioplasty. The long-term effects of such therapy, however, are still limited by an excessive arterial remodeling and restenosis^{1, 2}.

We have previously shown that extracellular RNA (eRNA) can exert prothrombotic and inflammatory properties in the vasculature. eRNA functions as a cofactor in protease auto-activation of contact-phase coagulation factors^{3, 4} and of Vascular Endothelial Growth factor (VEGF)- and VEGF-receptor2-coupled signaling pathways^{5, 6} and may induce cytokine mobilization and liberation from inflammatory cells⁷. Moreover, systemic treatment with RNase1 was shown to rescue mice from arterial thrombotic occlusion, to limit cerebral edema and infarct size after acute stroke, and to serve as a potent anti-inflammatory regimen *in vitro* and *in vivo*^{3, 5, 7-9}.

Based on these previous results and the contribution of eRNA to inflammatory processes, we have here investigated the role of eRNA in high-fat-diet induced atherosclerosis in low density lipoprotein receptor-deficient (*Ldlr*^{-/-}) mice and in a model of accelerated plaque formation in carotid arteries after injury in apolipoprotein E-deficient (*apoE*^{-/-}) mice.

Our new data provide strong evidence that eRNA-mediated reactions contribute to inflammation-driven processes in experimental atherosclerosis and vascular remodeling and that administration of RNase1 serves as a new intervention modality for the protection from atherogenesis.

Methods

Mouse models of atherosclerosis and intravital microscopy

Wild-type and *Ldlr*^{-/-} mice (both on the C57BL/6J background, $n=6$ per group) were obtained from the Jackson Laboratory (Bar Harbor, ME, USA), and *apoE*^{-/-} mice (C57BL/6J background, $n=13-14$ per group) from Charles River, Italy. *Ldlr*^{-/-} mice were fed an atherogenic diet as described¹⁰. *ApoE*^{-/-} mice, placed on an atherogenic high fat diet (HFD, 21% fat, 0.15% cholesterol) for one week before and up to three weeks after injury, were anaesthetized (100 mg/kg ketamine hydrochloride/ 10 mg/kg xylazine i.p.) and subjected to wire-induced arterial injury of the common carotid artery, as described^{11, 12}. Animals were treated intravenously with a bolus of 0.76 μg RNase1 (in PBS) or PBS alone immediately before arterial injury, and continuously treated with RNase1 via Alzet[®] osmotic minipumps

(42 µg/kg mouse per day), subcutaneously implanted one day before injury. Intravital microscopy was performed one day after injury as described¹¹. All animal studies were approved by local authorities and complied with German animal protection law.

Immunohistochemistry and quantification of RNA

5µm-thick cryosections of aortic sinus from *Ldlr*^{-/-} mice were used for RNA localization by staining with SYTO® RNASelect™ dye (Invitrogen)³ and visualizing with confocal microscopy (Nikon Eclipse TE2000-E, Nikon, Japan). Carotid arteries of *apoE*^{-/-} mice were excised and embedded in paraffin. Neointimal and medial areas were quantified in serial sections within 500 µm from the bifurcation by modified Movat's pentachrome staining and planimetry. Adjacent sections were used to assess cellular plaque content by immunofluorescence staining of Mac2⁺ macrophages and α-SMA⁺ SMC¹². For quantification of RNA, sections stained for SMC with TRITC-labeled antibody against smooth muscle α-actin, SYTO® RNASelect™ dye and DAPI were examined by laser scanning confocal microscopy (Leica TCS SP2). Each independent experiment represents the mean value of ten randomly chosen fields of vision in each section, quantified using three-dimensional "Quantification" and "VoxelShop" options of Imaris 6.3.1 (Bitplane). The area of specific labeling for eRNA was separately calculated as arbitrary fluorescent units of positive labeling per medial area or neointimal area, as previously described¹³.

RNase activity

At indicated time points, blood was taken from mice for analysis of RNase1 activity by an enzymatic assay, as described⁸. All activity values were normalized to the same protein concentration in different samples.

Isolation of eRNA and real time PCR analysis

DNA-free total RNA was extracted from serum of mice or cultured cell supernatants using the Zymo RNA MicroPrep kit (Zymo Research), including an additional DNA-digestion step. For real time PCR analysis, RNA was reverse-transcribed into cDNA at 37°C for 1 h (BioAnalyzer), and cDNA fragments were amplified using specific primer pairs (see Online Data Supplement for details).

Cell culture and cell adhesion assay under flow

Bone marrow-derived macrophages (BMDM) were generated from bone marrow cells in M-CSF-containing L929-conditioned medium as described^{10, 14}, or by incubation with mouse recombinant M-CSF or GM-CSF (50ng/ml each)¹⁵. Experiments were carried out for 24 h in 6-well trays (1.5 × 10⁶ cells/ml; Costar, Cambridge, MA) in the absence or presence of eRNA (1, 10 or 25 µg/ml), as indicated. Control cells were treated with growth medium alone (vehicle). For quantitation of TNF-α and Interleukin (IL)-6 protein production, BMDM were treated with eRNA (1, 10 or 25 µg/ml) for 24 h, followed by centrifugation and concentration of cell supernatants using centricon tubes (Millipore, Frankfurt, Germany) with a cutoff at 10 kDa. TNF-α and IL-6 ELISA were performed using commercially available kits from eBioscience (Frankfurt, Germany). Total protein concentration was determined using the BCA kit from Thermo-Fisher Scientific (Bonn, Germany). Human coronary artery SMC (Promocell) and MonoMac6 cells were maintained, as described^{11, 16}. MonoMac6 cell adhesion to SMC was analyzed in parallel wall flow-chambers¹¹. Confluent SMC were activated with eRNA (1, 10 or 25 µg/ml), or TNF-α (50 ng/ml) in the absence or presence of RNase1 (10 µg/ml) for 16 h.

Viability assay

Viability assays were performed after treating SMC and MonoMac6 cells with RNase1 (10 µg/ml) for 30 min or 16 h using the fluorescent CellTiter-Blue® cell viability assay (Promega, Mannheim, Germany).

Statistics

Data were analyzed by unpaired Student t tests or ANOVA 1-way analysis of variance followed by Tukey's or Dunnett's multiple comparison post-tests (detailed in the online Data Supplement). Differences with $p < 0.05$ were considered to be statistically significant.

Results

eRNA accumulates within lesions whereas plasma RNase activity decreases with the progression of atherosclerosis

The presence of eRNA was evaluated by immuno-histochemical staining in aortic root tissue from 8 week old *Ldlr*^{-/-} mice fed a chow diet and *Ldlr*^{-/-} mice fed a HFD for 8, 12 or 36 weeks in comparison to chow-fed B16 wild type mice. While no eRNA was detected in chow-fed B16 or *Ldlr*^{-/-} mice (RNA staining detectable in DAPI⁺ cell nuclei only), eRNA accumulated in atherosclerotic lesions of HFD-fed *Ldlr*^{-/-} mice in a time-progressive fashion (Figure 1). Quantification of eRNA showed a continuous increase in both the media and intima of *Ldlr*^{-/-} mice with increasing durations of HFD feeding; while relative staining for eRNA increased in the media exceeding that in the intima at early time points, eRNA was abundantly present predominantly in the intima at later time points, as reflected by an intense staining in this area (Figure 1, 2A). After 36 weeks of HFD, eRNA was detectable not only along the luminal lining and in the vicinity of lesional MOMA-2⁺ macrophages (Figure 1E, Figure 2B–E), but also within acellular necrotic core areas (Figure 1E, Figure 2F–K).

We further assessed RNA-degrading RNase activity in plasma samples from these mice during the course of HFD-feeding, and observed a biphasic characteristic with a temporary increase during the first 2 weeks (44 ± 9 vs. 70 ± 7 mU/mg protein; $p = 0.0012$), followed by a significant and sustained decrease to about 20–40% of the activity in baseline controls, starting at 4 weeks of HFD-feeding (44 ± 9 vs. 12 ± 2 mU/mg protein; $p < 0.0001$) (Figure 2L).

These data indicate that plasma RNase activity is enhanced in early atherosclerosis, but decreases during further plaque growth, when eRNA accumulates within atherosclerotic lesions in a time-progressive manner.

eRNA enhances cytokine secretion from macrophages

Given the association of eRNA with macrophages within atherosclerotic lesions, we assessed whether eRNA induces inflammatory responses in macrophages. Upon 24 h of stimulation of bone marrow-derived macrophages (BMDM) with eRNA *in vitro*, mRNA expression of pro-inflammatory cytokines *Tnf-α*, *Arg2*, *Il-1β*, *Il-6*, *Ifn-γ* was significantly upregulated in a concentration-dependent manner, while a reciprocal down-regulation of the anti-inflammatory cytokines *Il-10* and *Il-4* was observed (Figure 3A). Similarly, recombinant mouse M-CSF-driven BMDM-differentiation was skewed towards the M1-phenotype by exposure to eRNA, resulting in overexpression of inflammatory markers such as *Tnf-α*, *Arg2*, *Il-1β*, *Il-6*, *Ifn-γ* together with *Il-12* and inducible nitric oxide synthase (*iNOS*), whereas anti-inflammatory genes together with *Arg1* and macrophage mannose receptor-2 (*Cd206*) were significantly downregulated by eRNA (Figure 3B). The capacity of GM-CSF-driven BMDM-differentiation (already representing a M1-phenotype)^{15, 17}

towards further M1 polarization in response to eRNA was moderate; nevertheless, a significant down-regulation of M2 markers was confirmed (Supplementary Figure 1). In accordance with our proposal, these data clearly corroborate that self-eRNA serves as a pro-inflammatory alarming signal.

Accordingly, the release of TNF- α and IL-6 proteins into the cell supernatants was significantly increased by eRNA stimulation in a concentration-dependent manner (Figure 3C,D). We furthermore assessed whether these effects were mediated by eRNA-induced Toll-like receptor (TLR)-mediated signaling. Based on findings that no changes in *Stat1* expression were found in macrophages upon stimulation with eRNA (Figure 3A, B, and Supplementary Figure 1), we can conclude that eRNA does not engage in TLR-2 and TLR-4 signalling¹⁸. Likewise, no alterations in the mRNA expression of the cytokines studied were observed after poly-IC treatment (data not shown), indicating that also TLR-3 did not contribute to eRNA-mediated cytokine induction. Thus, eRNA functions as a powerful inducer of inflammatory cytokine responses in macrophages, independent of TLR-2, TLR-3 and TLR-4 signaling.

eRNA serves as damage marker in experimental atherosclerosis

To assess the functional role of eRNA in lesion growth, a model of injury-induced, accelerated atherosclerosis was employed. After injury, apolipoprotein E-deficient (*apoE*^{-/-}) mice displayed a marked increase in eRNA at 1 day and 1 week after injury (Figure 4A).

eRNA may be released from activated, damaged or necrotic cells during injury and is composed mainly of ribosomal RNA (about 85%), transfer RNA (about 10%) and mRNA (about 5%)^{4, 8}. We therefore determined the source of eRNA by analyzing the expression of specific mRNA species, indicative of the originating cell type. qPCR analysis revealed that both *Cd31* mRNA, employed as a marker for endothelial cells, as well as *α SMA* mRNA as a marker for SMC, were increased in plasma at day 1 but not immediately after injury (Figure 4B). These data indicate that endothelial cells and SMC release eRNA into the extracellular space during and after arterial injury.

Notably, eRNA was increased in supernatants of SMC in a time-dependent manner when cells were treated with TNF- α (Figure 4C), indicating that SMC may release eRNA also during cell activation.

Treatment of *apoE*^{-/-} mice with RNase1 diminishes experimental atherosclerosis

In order to investigate if eRNA directly or indirectly contributes to neointima formation after arterial injury, *apoE*^{-/-} mice fed a HFD and treated with RNase1 or vehicle (PBS) alone were subjected to wire-induced injury of the common carotid artery. RNase activity was markedly elevated in RNase1-treated mice, but not in control mice throughout the 3 week study period (Supplemental Figure 2). Moreover, RNase1 treatment inhibited the increase in eRNA (Figure 4A), and similarly diminished *Cd31* and *α SMA* mRNA appearance in plasma after injury compared to control-treated *apoE*^{-/-} mice (Figure 4B), confirming efficiency of the treatment.

Neointima formation was assessed at one and three weeks after injury, and revealed a trend towards reduced neointima formation at one week after injury and a significant reduction by 47 % after three weeks in RNase1-treated mice when compared to controls ($25.0 \pm 6.0 \times 10^3 \mu\text{m}^2$, n=8 mice, vs. $46.9 \pm 6.8 \times 10^3 \mu\text{m}^2$, n=7 mice, p=0.0136), whereas medial areas were diminished at one week week (32.0 ± 1.3 vs. $53.2 \pm 5.1 \times 10^3 \mu\text{m}^2$, n=3 mice each, p=0.0159) but remained unaltered at three weeks following injury (Figure 5A). This was

accompanied by a reduction in relative Mac-2⁺ macrophage plaque content (17.1 ± 4.4 vs. $61.2 \pm 7.6\%$, $p < 0.0001$) but an increase of α SMA⁺ SMC area at three weeks after injury (22.6 ± 1.9 vs. $15.4 \pm 4.2\%$, $p = 0.0339$) (Figure 5B,C), suggesting a reduction in mononuclear cell infiltration and a more stable plaque phenotype in RNase1-treated mice.

Importantly, a significant upregulation of *Tnf- α* and *Il-6* transcripts were observed at 1 day, 1 week and 3 weeks and of *Il-1 β* at 1 day and 1 week after injury compared to carotid arteries prior to injury, which was significantly reduced by RNase1 treatment (Figure 6A–C). Moreover, the injury-induced sustained induction of the adhesion molecules *Vcam-1*, *Icam-1*, *P-selectin* and *Ccl2* was abrogated in RNase1-treated mice (Figure 6D–G). In line, immunofluorescence staining of TNF- α and ICAM-1 protein in the arterial vessel wall, performed at 1 week after injury, was reduced in RNase1-treated mice (Figure 6H,I). These data demonstrate that the retardation in plaque growth induced by RNase-1 treatment was associated with a diminished expression of inflammatory cytokines and adhesion molecules in inflamed arteries *in vivo*.

eRNA mediates monocyte recruitment *in vitro* and in experimental atherosclerosis

It was previously shown that eRNA promotes leukocyte adhesion in the vasculature of the cremaster muscle and induces the expression of intracellular adhesion molecule-1 in endothelial cells *in vitro*⁷. Similarly, treatment of SMC with eRNA induced a mild but significant and concentration-dependent upregulation of the expression of *Vcam-1*, *Icam-1*, *P-selectin* and *Ccl2* with a maximal response at 10 μ g/mL (Supplemental Figure 3). To test whether eRNA may also facilitate monocyte recruitment to SMC, we monitored monocytic MonoMac6 cell adhesion to TNF- α -activated SMC. While MonoMac6 cells did not adhere to unstimulated SMC (not shown), MonoMac6 cell adhesion supported by activated SMC was significantly reduced when SMC were pretreated with RNase1; pretreatment of MonoMac6 cells did not affect cell adhesion per se (Figure 7A). Treatment with RNase1 did not consistently alter expression of adhesion molecules *Icam-1*, *Vcam-1*, *P-selectin* or *Ccl2* in untreated or TNF- α -activated SMC (not shown). Moreover, RNase1-pretreatment of untreated or TNF- α -stimulated MonoMac6 cells or SMC did not reduce cell viability (not shown). Thus, these collected data were not due to any direct changes in adhesion molecules in SMC or a cytotoxic effect of RNase1.

We further assessed whether eRNA may also contribute to leukocyte recruitment to injured arteries *in vivo*. To this end, intravital microscopy was performed one day after injury in carotid arteries of *apoE*^{-/-} mice, treated with vehicle (PBS) only in comparison to RNase1 administration. Notably, leukocyte adhesion to injured artery segments was substantially reduced in RNase1-treated *apoE*^{-/-} mice compared to vehicle-treated mice (14.6 ± 1.7 cells/HPF, $n = 6$ mice, vs. 8.2 ± 2.3 cells/HPF, $n = 7$ mice, $p = 0.0491$) (Figure 7B). These findings indicate that eRNA accumulation following injury may directly or indirectly (e.g. via TNF- α) contribute to leukocyte recruitment and plaque formation *in vivo*.

Discussion

In the present study the multifunctional eRNA/RNase system was characterized for its contribution to chronic vascular disease as it relates to the progression of atherosclerotic lesion formation in two established mouse models. Our data indicate that (i) in *Ldlr*^{-/-} mice fed a HFD, eRNA accumulates in atherosclerotic plaques in a time-dependent manner, can be released from activated cells, and is increased in plasma of *apoE*^{-/-} mice after arterial injury; (ii) conversely, a biphasic characteristic for plasma RNase activity was observed with an increase soon after the initiation of HFD, and a decline to levels below baseline during progressive plaque growth; (iii) eRNA induces an inflammatory gene expression in bone-marrow-derived macrophages and increases adhesion molecular expression in SMC, and (iv)

promotes monocyte adhesion to activated SMC *in vitro* and to the carotid vessel wall *in vivo*; (v) RNase1 administration in HFD-fed *apoE*^{-/-} mice results in significantly reduced neointimal plaque formation, monocyte recruitment and vascular inflammation after injury. Together, these data provide strong evidence for a major role of the extracellular RNA/RNase system in atherogenesis and establish RNase1-treatment as a potential novel therapeutic regimen.

We here for the first time demonstrate that eRNA accumulates within arterial lesions in the media and at later stages predominantly in the neointima in a time-dependent fashion, as documented by staining of affected vascular sites with an RNA-binding dye in HFD-fed mice, but not in controls. Furthermore, we evidenced an increased eRNA content in plasma after arterial injury *in vivo*. This may be due to the direct release of RNA from damaged tissues, as mRNA (as a portion of eRNA) originating from endothelial cells and SMC was elevated as well. The TNF- α -induced increase in eRNA released from cultured SMC furthermore implied that RNA may also be released from cells in the context of inflammation and cytokine exposure after injury. Conversely, we recently demonstrated that eRNA may increase the extracellular concentration of TNF- α by promoting the liberation of transmembrane pro-TNF via the sheddase TACE⁷, such that both reactions may amplify the concentration of TNF- α and other cytokines.

Although eRNA may be degraded by plasma RNases, increased levels of eRNA were similarly detected in tumor patients, sepsis or lung fibrosis^{4, 8}. This led us to propose that eRNA, released under pathological conditions, may become protected against degradation by binding to proteins and phospholipids¹⁹, or is associated with microparticles or exosomes²⁰. However, the biphasic change of vascular RNases, showing an increase early after the initiation of a HFD-diet, but a decrease in the course of chronic lesion formation (observed from 4 weeks on), strongly implies a causal relationship between a dysbalance in the eRNA/RNase system and the initiation and progression of atherosclerosis. No significant changes in RNase activity were noted between wild type, *Ldlr*^{-/-} and *apoE*^{-/-} mice (not shown). However, no regulation in RNase activity was noted in *apoE*^{-/-} mice in the accelerated model of injury-induced atherosclerosis, suggesting that injury-associated factors, such as a massive release of RNA from damaged cells, may have either consumed the atherosclerosis-induced early increase in RNase activity or abrogated its induction.

In accordance with the damaging nature of eRNA, several pro-inflammatory cytokines (including TNF- α , IL-1 β , IL-6) were upregulated in macrophages, whereas a decrease in anti-inflammatory cytokines was demonstrated: This is in line with a shift in macrophage polarization towards the M1-phenotype, as well as a repression of typical M-2 phenotype markers such as Arg1 or CD206. No involvement of TLRs in self eRNA-cell interactions was noted. Importantly, the indicated inflammatory cytokines were also increased in carotid arteries after injury *in vivo*, while RNase1 treatment significantly reduced their expression levels compared to controls. In essence, the appearance of eRNA in the diseased tissue may thus be considered as an alarm signal that amplifies tissue inflammation by the induction of cytokine production, and promotion of M1-macrophage polarization as well as by releasing bioactive TNF- α , as documented earlier⁷, being a potent pro-atherogenic factor¹⁶. The latter process may involve direct or indirect activation of TNF- α -converting enzyme by eRNA, as previously demonstrated by our group²¹.

Recently, it was revealed that eRNA not only promotes the adhesion and transmigration of leukocytes in the murine cremaster muscle vasculature, but that it also induces the expression of ICAM-1 in endothelial cells *in vitro*⁷. Similarly, we here observed an increase in adhesion molecules ICAM-1, VCAM-1, P-Selectin and CCL2 in SMC, which may likewise contribute to monocyte adhesion to activated SMC as well as to leucocyte

recruitment in carotid arteries after injury²². Importantly, and in line with a pro-inflammatory function of eRNA, our findings show that the systemic treatment with RNase1 reduced adhesion molecule expression, inhibited leukocyte adhesion and reduced arterial macrophage accumulation and neointimal plaque formation after injury in carotid arteries of *apoE^{-/-}* mice *in vivo*.

eRNA was also demonstrated to mediate vascular permeability via the mobilization/stabilization and direct binding to vascular endothelial growth factor⁵. Enhanced vascular endothelial growth factor signaling induced by eRNA may in addition promote monocyte adhesion and plaque expansion²³.

In addition, eRNA was shown to act as a pro-thrombotic cofactor. Accordingly, systemic treatment with RNase1 rescued mice from thrombotic occlusion of the carotid artery in a model of arterial thrombosis³, and reduced cerebral edema and infarction size in acute stroke⁹. Neointimal hyperplasia after arterial injury is characterized by endothelial denudation, exposure of extracellular matrix, and adhesion of activated platelets, which all contribute to inflammatory leukocyte recruitment and neointima formation after injury²⁴. By contributing to platelet accumulation at the site of injury, eRNA may thus in addition promote injury-induced leukocyte adhesion and neointimal hyperplasia.

The underlying pathogenetic mechanisms of eRNA as a pro-inflammatory mediator may thus involve both direct and indirect signaling pathways. Our findings thus indicate that eRNA serves as an important inflammatory mediator after vascular injury, identifying extracellular ribonucleic acids as a new target for the treatment of inflammation during vascular remodeling.

Together, the present study provides novel experimental evidence for the multifunctional properties of self-eRNA as an important trigger of different inflammatory processes that fuel atherogenesis and may culminate in atherosclerotic lesion growth. Our experimental data that administration of RNase1 abrogates the detrimental functions of eRNA provides promising evidence for the establishment of novel interventional strategies for the therapy of cardiovascular diseases.

Supplementary Material

Refer to Web version on PubMed Central for supplementary material.

Acknowledgments

We thank Stephanie Elbin, Melanie Garbe, Roya Soltan and Sara McCurdy for excellent technical assistance.

Funding Sources: This work was in part supported by the Deutsche Forschungs-gemeinschaft: FOR809, ZE-827/1-2, ZE-827/4-1 and SFB688 TPA12 to A.Z.; PROMISE-IRTG-1566 and the Excellence Cluster Cardiopulmonary System to K.T.P.; NIH grants HL75677 and HL081863, and Hawaii Community Foundation grant 47037 to W.A.B. Core facilities at the University of Hawaii were supported by P30GM103341. We are grateful for the support of a stipend (lab-rotation fellowship) from the “International Giessen-Graduate Center for the Life Sciences” (GGL) as well as by the Giessen-Kazan Partnership (Deutscher Akademischer Austauschdienst (DAAD; Bonn, Germany) to H.A.C.F.

References

1. Weber C, Noels H. Atherosclerosis: Current pathogenesis and therapeutic options. *Nat Med.* 2011; 17:1410–1422. [PubMed: 22064431]
2. Inoue T, Croce K, Morooka T, Sakuma M, Node K, Simon DI. Vascular inflammation and repair: Implications for re-endothelialization, restenosis, and stent thrombosis. *JACC Cardiovasc Interv.* 2011; 4:1057–1066. [PubMed: 22017929]

3. Kannemeier C, Shibamiya A, Nakazawa F, Trusheim H, Ruppert C, Markart P, Song Y, Tzima E, Kennerknecht E, Niepmann M, von Bruehl ML, Sedding D, Massberg S, Gunther A, Engelmann B, Preissner KT. Extracellular rna constitutes a natural procoagulant cofactor in blood coagulation. *Proc Natl Acad Sci U S A*. 2007; 104:6388–6393. [PubMed: 17405864]
4. Fischer S, Preissner KT. Extracellular nucleic acids as novel alarm signals in the vascular system. *Mediators of defence and disease. Hamostaseologie*. 2013; 33:37–42. [PubMed: 23328880]
5. Fischer S, Gerriets T, Wessels C, Walberer M, Kostin S, Stolz E, Zheleva K, Hocke A, Hippenstiel S, Preissner KT. Extracellular rna mediates endothelial-cell permeability via vascular endothelial growth factor. *Blood*. 2007; 110:2457–2465. [PubMed: 17576819]
6. Fischer S, Nishio M, Peters SC, Tschernatsch M, Walberer M, Weidemann S, Heidenreich R, Couraud PO, Weksler BB, Romero IA, Gerriets T, Preissner KT. Signaling mechanism of extracellular rna in endothelial cells. *Faseb J*. 2009; 23:2100–2109. [PubMed: 19246491]
7. Fischer S, Grantzow T, Pagel JI, Tschernatsch M, Sperandio M, Preissner KT, Deindl E. Extracellular rna promotes leukocyte recruitment in the vascular system by mobilising proinflammatory cytokines. *Thromb Haemost*. 2012; 108:730–741. [PubMed: 22836360]
8. Fischer S, Nishio M, Dadkhahi S, Gansler J, Saffarzadeh M, Shibamiyama A, Kral N, Baal N, Koyama T, Deindl E, Preissner KT. Expression and localisation of vascular ribonucleases in endothelial cells. *Thromb Haemost*. 2011; 105:345–355. [PubMed: 21103661]
9. Walberer M, Tschernatsch M, Fischer S, Ritschel N, Volk K, Friedrich C, Bachmann G, Mueller C, Kaps M, Nedelmann M, Blaes F, Preissner KT, Gerriets T. Rnase therapy assessed by magnetic resonance imaging reduces cerebral edema and infarction size in acute stroke. *Curr Neurovasc Res*. 2009; 6:12–19. [PubMed: 19355922]
10. Han X, Kitamoto S, Wang H, Boisvert WA. Interleukin-10 overexpression in macrophages suppresses atherosclerosis in hyperlipidemic mice. *Faseb J*. 2010; 24:2869–2880. [PubMed: 20354139]
11. Shagdarsuren E, Bidzhekov K, Djalali-Talab Y, Liehn EA, Hristov M, Matthijsen RA, Buurman WA, Zernecke A, Weber C. C1-esterase inhibitor protects against neointima formation after arterial injury in atherosclerosis-prone mice. *Circulation*. 2008; 117:70–78. [PubMed: 18071075]
12. Shagdarsuren E, Djalali-Talab Y, Aurrand-Lions M, Bidzhekov K, Liehn EA, Imhof BA, Weber C, Zernecke A. Importance of junctional adhesion molecule-c for neointimal hyperplasia and monocyte recruitment in atherosclerosis-prone mice-brief report. *Arterioscler Thromb Vasc Biol*. 2009; 29:1161–1163. [PubMed: 19520977]
13. Cai W, Vosschulte R, Afsah-Hedjri A, Koltai S, Kocsis E, Scholz D, Kostin S, Schaper W, Schaper J. Altered balance between extracellular proteolysis and antiproteolysis is associated with adaptive coronary arteriogenesis. *J Mol Cell Cardiol*. 2000; 32:997–1011. [PubMed: 10888253]
14. Han X, Kitamoto S, Lian Q, Boisvert WA. Interleukin-10 facilitates both cholesterol uptake and efflux in macrophages. *J Biol Chem*. 2009; 284:32950–32958. [PubMed: 19776020]
15. Neu C, Sedlag A, Bayer C, Forster S, Crauwels P, Niess JH, van Zandbergen G, Frascaroli G, Riedel CU. Cd14-dependent monocyte isolation enhances phagocytosis of listeria monocytogenes by proinflammatory, gm-csf-derived macrophages. *PloS one*. 2013; 8:e66898. [PubMed: 23776701]
16. Weber C, Aepfelbacher M, Haag H, Ziegler-Heitbrock HW, Weber PC. Tumor necrosis factor induces enhanced responses to platelet-activating factor and differentiation in human monocytic mono mac 6 cells. *Eur J Immunol*. 1993; 23:852–859. [PubMed: 7681399]
17. Tugal D, Liao X, Jain MK. Transcriptional control of macrophage polarization. *Arterioscler Thromb Vasc Biol*. 2013; 33:1135–1144. [PubMed: 23640482]
18. Rhee SH, Jones BW, Toshchakov V, Vogel SN, Fenton MJ. Toll-like receptors 2 and 4 activate stat1 serine phosphorylation by distinct mechanisms in macrophages. *J Biol Chem*. 2003; 278:22506–22512. [PubMed: 12686553]
19. Wiczorek AJ, Rhyner C, Block LH. Isolation and characterization of an rna-proteolipid complex associated with the malignant state in humans. *Proc Natl Acad Sci U S A*. 1985; 82:3455–3459. [PubMed: 2582412]

20. Ekström K, Valadi H, Sjöstrand M, Malmhäll C, Bossios A, Eldh M, Lötval J. Characterization of mrna and microrna in human mast cell-derived exosomes and their transfer to other mast cells and blood cd34 progenitor cells. *J Extracell Vesicles*. 2012:1–12.
21. Fischer S, Gesierich S, Griemert B, Schanzer A, Acker T, Augustin HG, Olsson AK, Preissner KT. Extracellular rna liberates tumor necrosis factor-alpha to promote tumor cell trafficking and progression. *Cancer Res*. 2013; 73:5080–5089. [PubMed: 23774209]
22. Manka DR, Wiegman P, Din S, Sanders JM, Green SA, Gimple LW, Ragosta M, Powers ER, Ley K, Sarembock IJ. Arterial injury increases expression of inflammatory adhesion molecules in the carotid arteries of apolipoprotein-e-deficient mice. *J Vasc Res*. 1999; 36:372–378. [PubMed: 10559677]
23. Lucerna M, Zerneck A, de Nooijer R, de Jager SC, Bot I, van der Lans C, Kholova I, Liehn EA, van Berkel TJ, Yla-Herttuala S, Weber C, Biessen EA. Vascular endothelial growth factor-a induces plaque expansion in apoe knock-out mice by promoting de novo leukocyte recruitment. *Blood*. 2007; 109:122–129. [PubMed: 16990600]
24. Schober A, Manka D, von Hundelshausen P, Huo Y, Hanrath P, Sarembock IJ, Ley K, Weber C. Deposition of platelet rantes triggering monocyte recruitment requires p-selectin and is involved in neointima formation after arterial injury. *Circulation*. 2002; 106:1523–1529. [PubMed: 12234959]

Clinical perspective

Atherosclerosis remains the number one cause of death in the Western world, and the therapeutic options currently available are limited. Regarded as a chronic inflammatory disease of the vessel wall, monocytes/macrophages, inflamed smooth muscle cells as well several cytokines, proteases and other molecular players contribute to disease development. Based on our previous studies concerning extracellular RNA (eRNA) as a novel alarm signal and potent cofactor in inflammation and thrombosis, we here investigated the contribution of the eRNA/RNase system during atherogenesis. In the experimental model of high-fat-diet induced atherosclerosis in LDL-receptor-deficient and apolipoprotein E-deficient mice, eRNA accumulated in atherosclerotic plaques in a time-dependent manner, but was also released from activated cells, yielding increased plasma levels after arterial injury. In fact, eRNA functioned to promote inflammatory gene expression in macrophages and smooth muscle cells. Importantly, eRNA-degrading RNase1, administered via minipumps, significantly reduced plaque formation, monocyte recruitment and vascular inflammation after injury. These data provide evidence for a major role of the extracellular RNA/RNase system in atherogenesis and identify eRNA as an important trigger of inflammatory processes that fuel atherosclerotic lesion growth. These novel data extend our previous findings where RNase1 was found to reduce infarction size in acute stroke. Thus, our study may harbor great potential for the establishment of RNase1 administration as a novel interventional strategy for the therapy of cardiovascular diseases. Since RNase1 is a thermo-stable, non-toxic enzyme, it bears several features to be applicable as new interventional regimen against atherothrombotic disease.

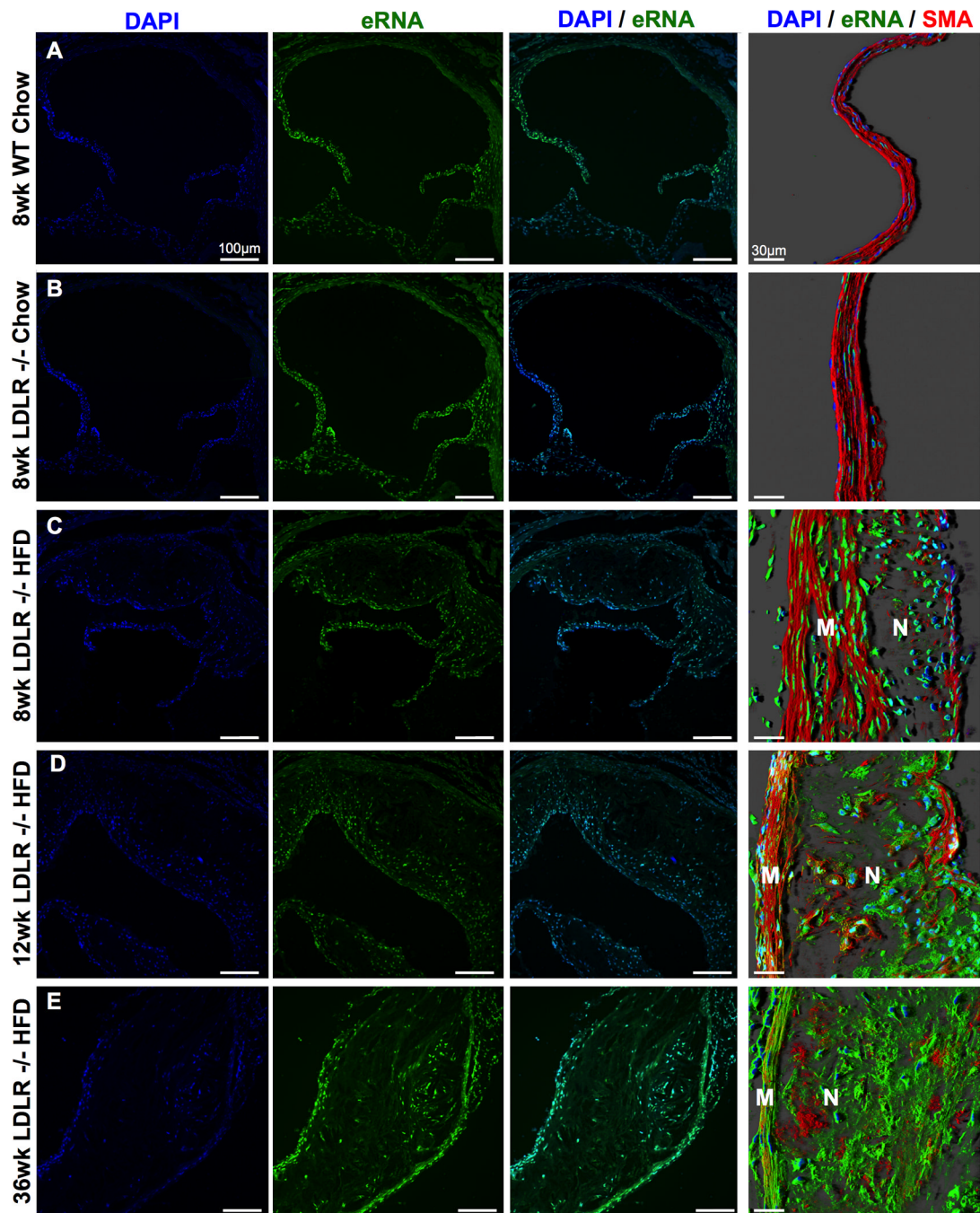


Figure 1.

Time-progressive distribution of extracellular RNA (eRNA) in atherosclerotic lesions. The presence of eRNA in aortic root tissue from WT or *Ldlr*^{-/-} mice fed a chow diet for 8 weeks or from *Ldlr*^{-/-} mice fed a high-fat-diet (HFD) for 8 (A-C), 12 (D) or 36 weeks (E), as indicated, was demonstrated by confocal microscopy using an RNA-binding fluorescence dye (RNA-Select, green) together with cell nuclei staining (DAPI, blue). Right panel in each line: confocal images with merged immunostaining for eRNA (green), cell nuclei (DAPI, blue) and smooth muscle cell actin (SMA, red); M: media; N: neointima. (n=6 per group).

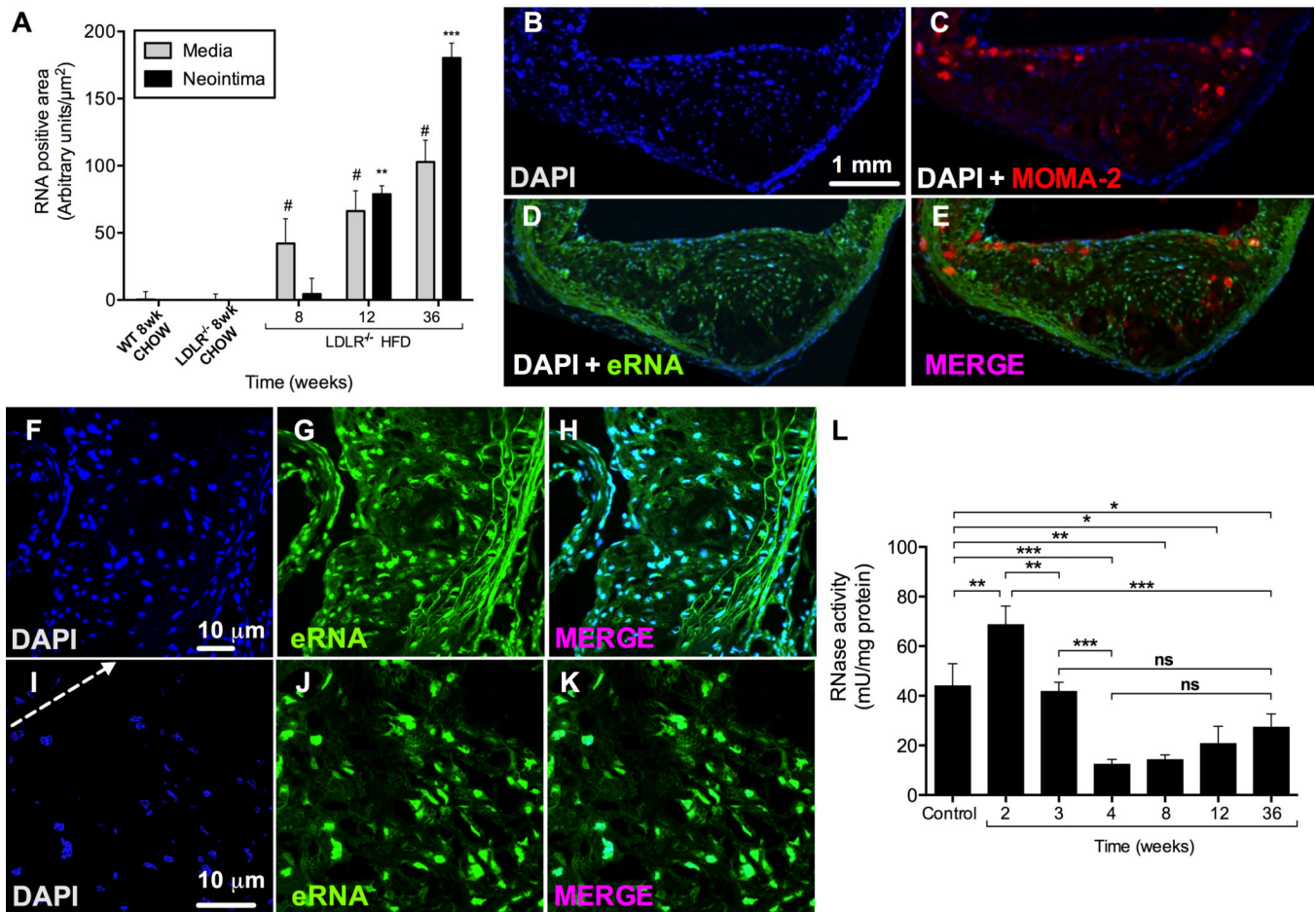


Figure 2.

Co-localization of eRNA and macrophages in atherosclerotic lesions of *Ldlr*^{-/-} mice after 36 weeks on HFD, and RNase activity in mouse plasma. (A) Quantitative analysis of eRNA-associated fluorescence intensity in aortic root tissue in the media and neointima in wild-type (WT) and *Ldlr*^{-/-} mice fed a normal chow or high fat diet for indicated time periods. Values are expressed as mean \pm SD (n=6 per group); #p<0.05 vs. media, and **p<0.001 vs. neointima in chow-fed *Ldlr*^{-/-} mice. (B-E) Immunofluorescence staining in cryosections of atherosclerotic lesions from *Ldlr*^{-/-} mice after 36 weeks on HFD. Staining for eRNA (D) was performed by an RNA-binding fluorescence dye (RNA-Select, green), macrophages (C) were identified by the anti-MOMA-2 monoclonal antibody (red), and cell nuclei (B) were marked by DAPI staining (blue). (E-K) Higher magnifications of atherosclerotic lesions are shown stained with DAPI (blue, F,I; arrow indicates cellular towards acellular necrotic core regions) and RNA-binding fluorescence dye (green, G,J); merged images are indicated in (H,K). All images were obtained under identical conditions of confocal laser beam intensity and exposure time; representative images are displayed (n=4). (L) RNase activity in *Ldlr*^{-/-} mouse plasma was quantified for each time point and normalized to plasma protein concentration. Values are expressed as mean \pm SD (n=6–12 per group); ns=non-significant, *p<0.05, **p<0.01, ***p<0.001.

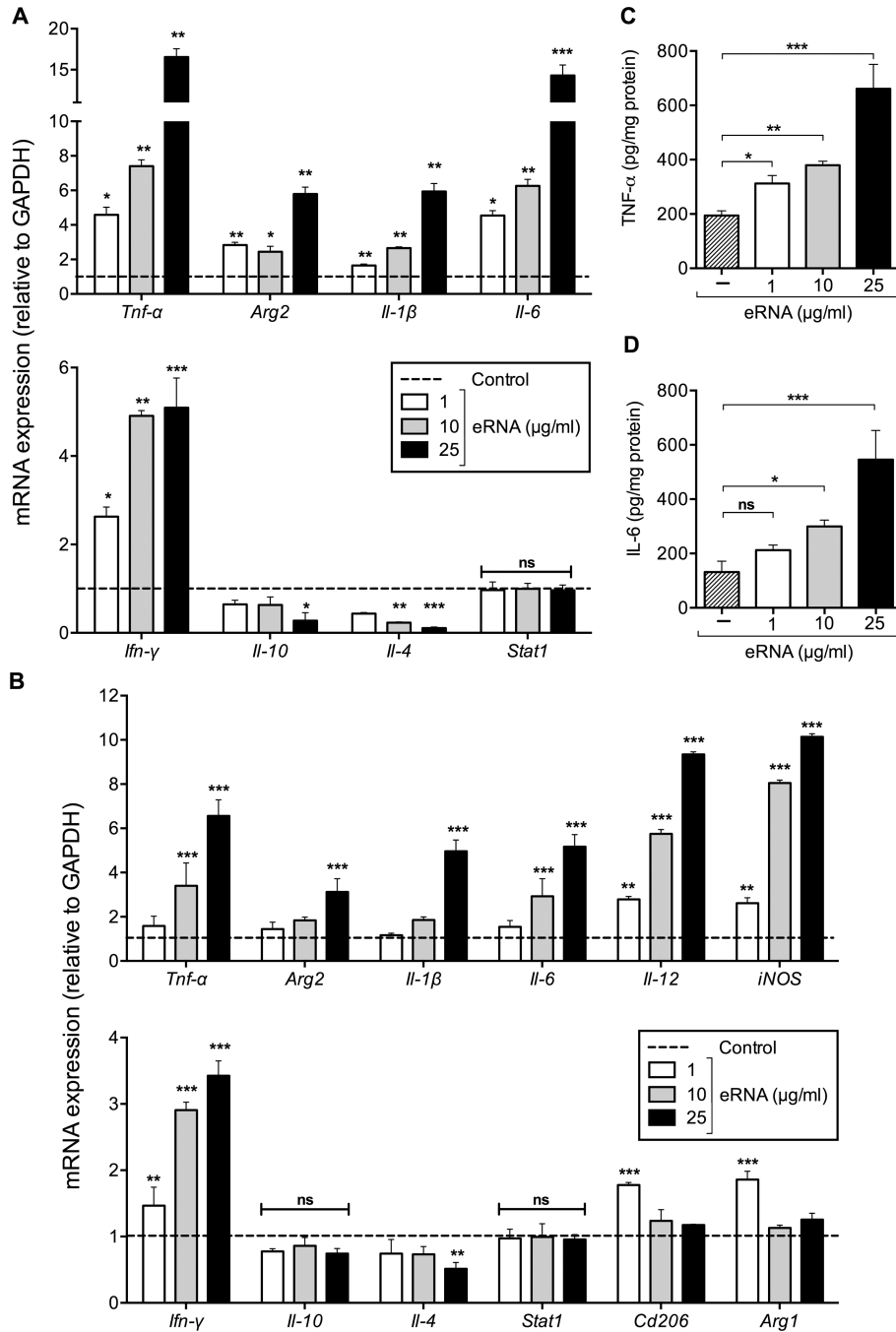


Figure 3. Influence of extracellular RNA on pro- and anti-inflammatory mediators in bone marrow-derived macrophages (BMDM). (A) mRNA expression of *Tnf-α*, *Arg2*, *Il-1β*, *Il-6*, *Ifn-γ*, *Il-10*, *Il-4* and *Stat1* in wild-type BMDM, differentiated in the presence of M-CSF-containing L929-conditioned medium was analyzed by real-time PCR in the absence (control, dotted line) or presence of eRNA (1, 10, or 25 μg/ml) for 24 h. Data are expressed as changes in the ratio between target gene expression and *Gapdh* mRNA. Values represent mean ± SD (n=6 per group); *p<0.05, **p<0.01, ***p<0.001 vs. control, ns = non-significant. (B) mRNA expression of *Tnf-α*, *Arg2*, *Il-1β*, *Il-6*, *Il-12*, *iNOS*, *Ifn-γ*, *Il-10*, *Il-4*,

Stat1, *Cd206* and *Arg1* in wild-type BMDM, differentiated in the presence of mouse recombinant M-CSF was analyzed by real-time PCR in the absence (control, dotted line) or presence of eRNA (1, 10, or 25 µg/ml) for 24 h. Data are expressed as changes in the ratio between target gene expression and *Gapdh* mRNA. Values represent mean ± SD (n=6 per group); *p<0.05, **p<0.01, ***p<0.001 vs. control, ns = non-significant. (C) TNF-α or (D) IL-6 protein concentration was measured in the supernatants of BMDM following treatment in the absence (control) or presence of eRNA (1, 10, or 25 µg/ml) as indicated. Values correspond to mean ± SD (n=9 per group). *p<0.05, **p<0.01, ***p<0.001, ns=non-significant.

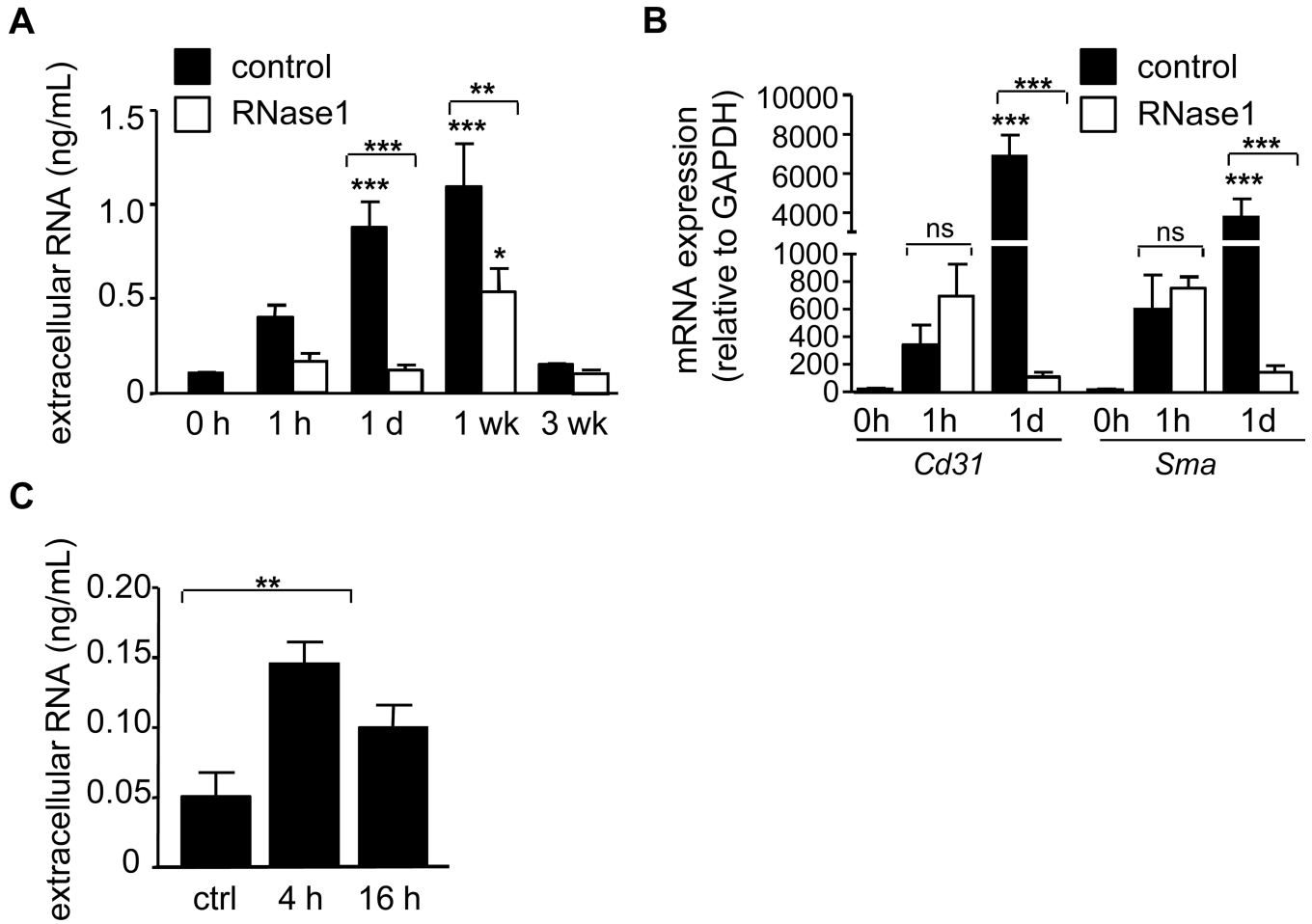


Figure 4. eRNA increases after vascular injury. (A) The concentration of eRNA in plasma of *apoE*^{-/-} mice before injury (0 h) and at indicated time points after arterial injury was measured in the control (filled bars) and the RNase1-treatment group (open bars). Values are expressed as mean ± SEM (n=7 per group). *p<0.05, **p<0.01, ***p<0.001 vs. 0h control, or as indicated. (B) mRNA detection for *Cd31* (endothelial cells) and α -smooth muscle actin (*Sma*, smooth muscle cells) in plasma before injury (0h), at 1 h and 1 day after injury (n=4–5 per group) was quantified by real-time PCR in the control (filled bars) and RNase1-treatment group (open bars). Values are expressed as mean ± SEM; *p<0.05, **p<0.01, and ***p<0.001 vs. 0h, or as indicated; ns=non-significant. (C) Extracellular RNA concentration was measured in supernatants of SMC activated with TNF- α for 4 h or 16 h. Values represent mean ± SEM (n=6 per group); *p<0.05.

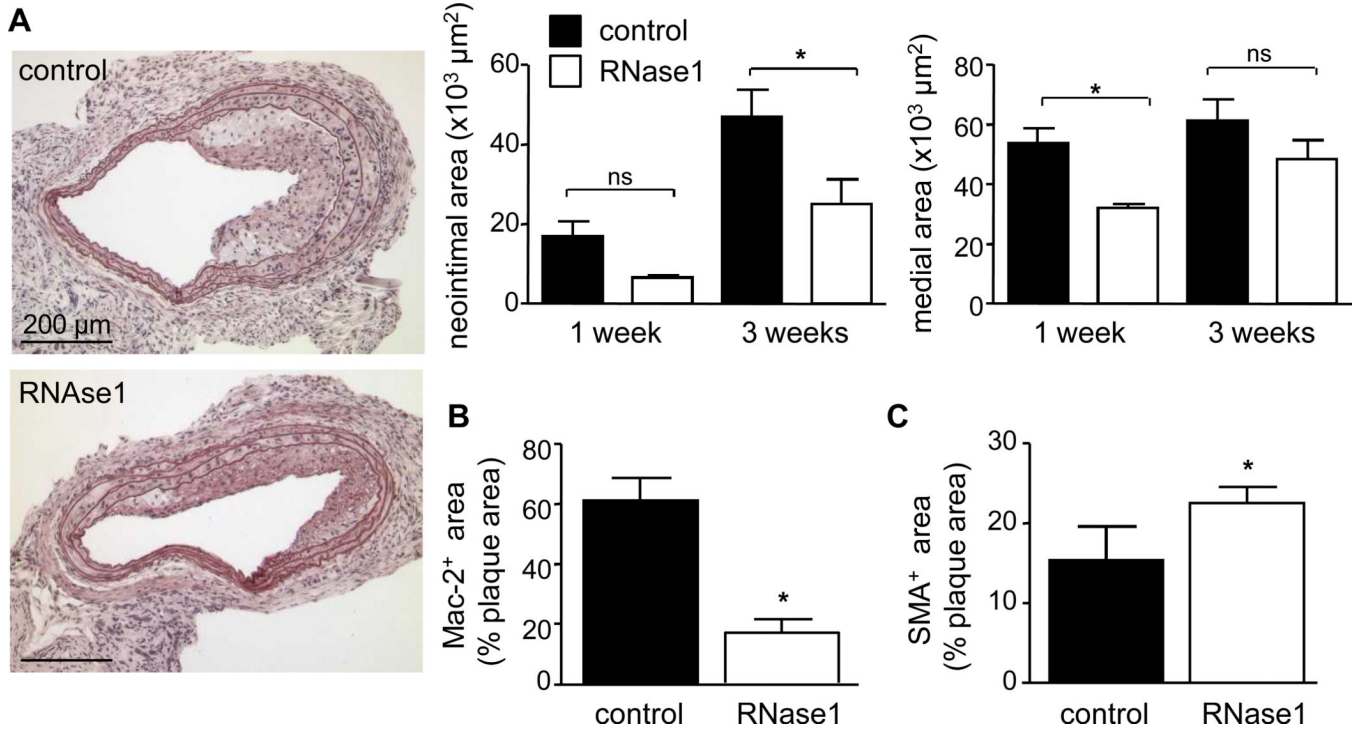


Figure 5. RNase1 treatment of atherosclerosis-prone *apoE*^{-/-} mice protects from neointimal plaque formation. (A-C) *ApoE*^{-/-} mice fed a high fat diet and treated vehicle (PBS, filled bars) or RNase1 (open bars) were subjected to wire-induced injury of the common carotid artery. Neointimal and medial areas were assessed 1 week (n=3 per group) and 3 weeks (n=7–8 per group) after injury. Values represent mean ± SEM; *p<0.05; ns = non-significant. Representative images of pentachrome-stained sections at 3 weeks after injury are documented (A). Quantification of the relative content of Mac-2-positive neointimal macrophages (B) as well as α-SMA-positive SMC (C) are indicated in the control group (filled bars) as compared to the RNase1-treatment group (open bars) 3 weeks after injury. Values represent mean ± SEM; *p<0.05.

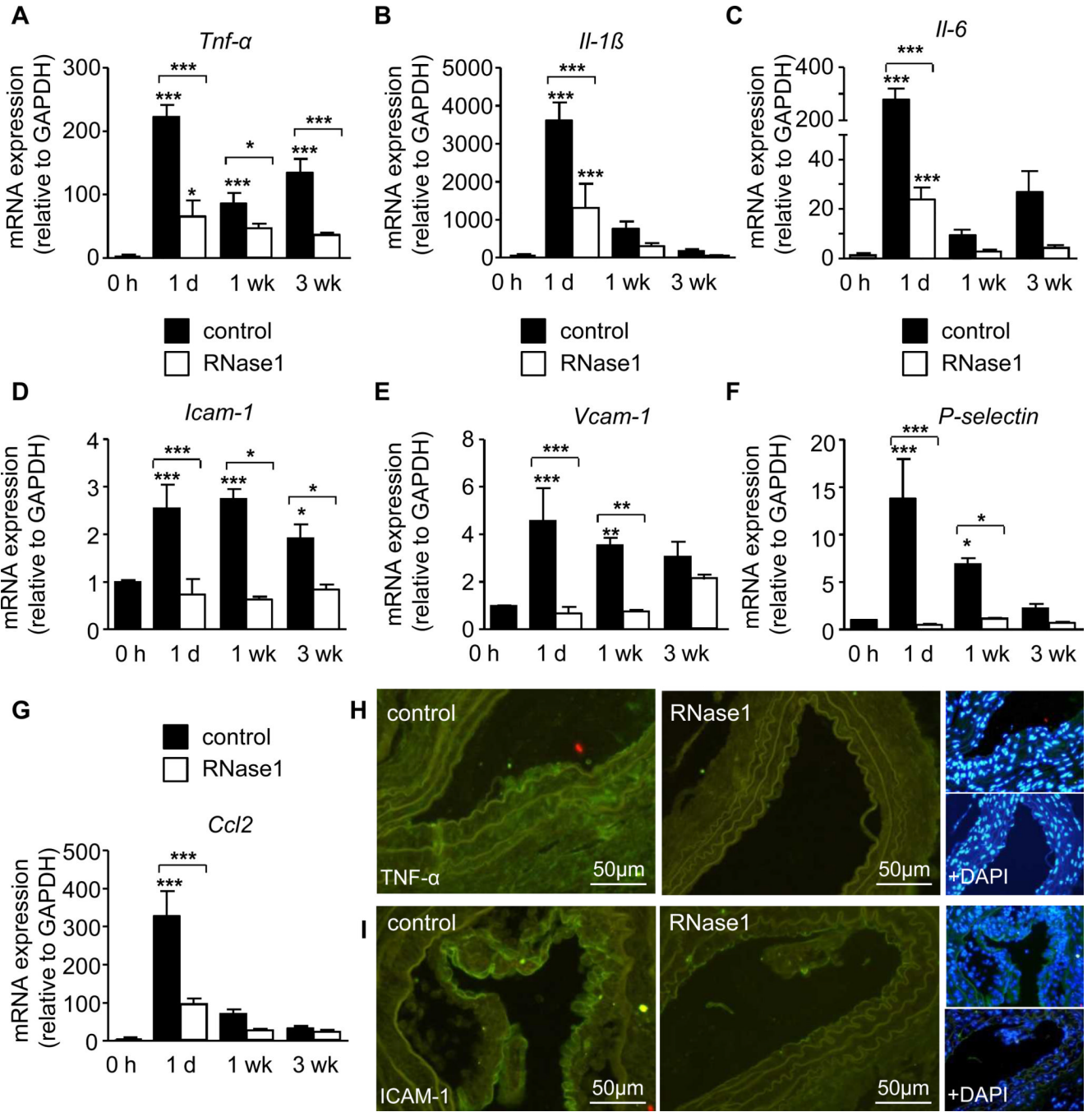


Figure 6. RNase1 treatment of atherosclerosis-prone *apoE*^{-/-} mice reduces vascular cytokine and adhesion molecule expression. (A-I) *ApoE*^{-/-} mice fed a high fat diet and treated with vehicle (PBS, filled bars) or RNase1 (open bars) were subjected to wire-induced injury of the common carotid artery. *Tnf-α* (A), *Il-1β* (B) and *Il-6* (C), *Icam-1* (D), *Vcam-1* (E), *P-selectin* (F) and *Ccl2* (G) mRNA expression were assessed at indicated time points after injury. Data are expressed as changes in the ratio between target gene expression and *Gapdh* mRNA. Values represent mean ± SEM (n=12 per group); *p<0.05, **p<0.01, and ***p<0.001 vs. 0h, or as indicated. (H,I) Representative fluorescence images of TNF-α (H)

and ICAM-1 (I) protein expression (green) at 1 week after injury, and together with cell nuclei staining (DAPI, blue).

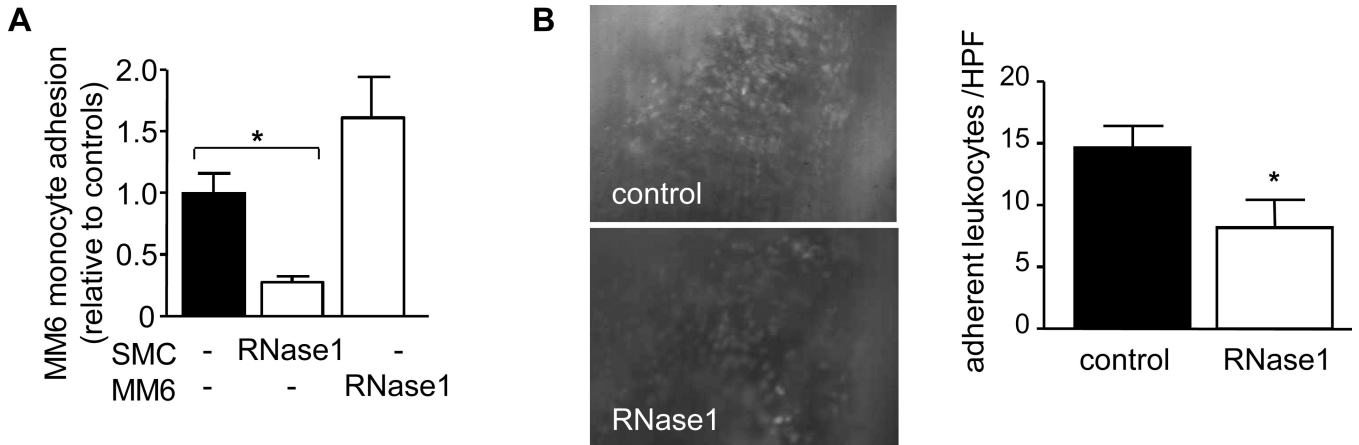


Figure 7. eRNA contributes to monocyte adhesion to activated SMC and carotid arteries after injury. (A) MonoMac 6 cell adhesion to TNF- α -activated SMC was analyzed under flow conditions *in vitro* in the absence (filled bar) or presence of RNase1 (open bars), as indicated. Values represent mean \pm SEM (n=6–8 per group). *p<0.05. (B) Leukocyte adhesion to carotid arteries of *apoE*^{-/-} mice treated with vehicle (control) or RNase1 one day after injury *in vivo* (n=6–7 per group) was determined. Representative images of rhodamine 6G-labeled leukocytes adhering to carotid arteries (original magnification \times 20) as well as quantitation of results are shown. Values represent mean \pm SEM; *p<0.05.